

Innovative filtration system based on silver activated sand combined with adsorption processes to remove water borne bacteria.

Daniel K. Arusei^{1*} Prof. Charles Nzila² Prof. Emmanuel Kipkorir³

1. Department of Mechanical and Production Engineering, Moi University, 3900-30100 Eldoret Kenya
 2. Department of Manufacturing, Industrial and Textile Engineering, Moi University, 3900-30100 Eldoret Kenya
 3. Department of Civil and Structural Engineering, Moi University, 3900-30100 Eldoret Kenya
- * E-mail of the corresponding author: aruseid@gmail.com

The research was financed by African Centre of Excellence in Phytochemicals, Textiles and Renewable Energy (ACEII-PTRE)

Abstract

Waterborne diseases significantly contribute to illness and death among children under five in Kenya. This is primarily due to insufficient and affordable infrastructure for water treatment. The majority of the water in Kenya fails to comply with drinking water standards established by KEBS and WHO, thereby posing a risk for waterborne diseases. To guarantee safe and readily available drinking water for everyone by the year 2030 as per SDG 6, it is essential to invest in proper affordable water treatment infrastructure, provide sanitation facilities, and encourage good hygiene practices. Domestic water treatment at point of use, is a crucial engineering intervention to address daily and emergency domestic water supply requirements. Traditional and conventional HWT methods have inherent technical and economic limitations that make HWT unsustainable, the study is premised on innovative and unique method of water treatment by utilizing silver activated sand to develop a device capable of treating water to meet KEBS and WHO requirements of drinking water. This study aimed to design, construct, and evaluate the performance of a domestic activated sand purification device for removal of physical, chemical and biological contaminants from polluted water. The activated sand used is a sand-type catalytic disinfectant mainly composed of silica, aluminum silicate, silver, Iron and copper. The physical and chemical properties of the filter material were investigated using X-ray fluorescence (XRF), microscopic and Fourier transform infrared spectroscopy (FTIR). Leaching of silver into the effluent was conducted through Atomic absorption Spectroscopy (AAS). Water quality parameters were conducted using standard methods and equipment. Through iterative design process the optimum design was a multi-layered filter media consisting of five layers packed to facilitate the removal of pollutants at each layer. Biological removal efficiencies were 100% for Salmonella, 100% for Shigella, 100% for *S. faecalis*, 99.9% for total coliform bacteria, and 99% for filter cartridges 1 and 2, respectively. The results clearly demonstrate that the silver-activated water purification system provides an effective and sustainable solution for improving domestic water quality by utilizing the antimicrobial properties of silver. This system addresses significant public health problems associated with waterborne diseases.

Keywords: Household, drinking water, Point of use, Salmonella, Shigella, Coliforms, *S.faecalis*

DOI: 10.7176/JEES/14-6-02

Publication date: December 30th 2024

1.Introduction

Statistics show that, 2.2 billion people around the globe, mostly located in low- and middle- income countries, have no potable water situated on premises, available when needed, or free from contamination (*Drinking Water FactSheet*, 2019). Recent studies also highlight a high population without safely managed potable water services in developed countries. Kenya with a population of 50 million, 32 percent of Kenyans rely on unimproved water sources, such as ponds, shallow wells and rivers which are prone to chemical, thermal and physical contamination ("water.org/," 2021). Most water in Kenya do not meet the threshold for potable water standards set by KEBS and WHO and therefore can be potential sources of water-borne diseases (Sila, 2018). Even where

water is safe at the source, unless protected by residual disinfection or improved storage, it is frequently subject to extensive recontamination during collection, storage and household use (Wright, 2003). The United Nations Sustainable Development Goal (SDG) 6, clean water and sanitation, sets various targets to make water sustainable for use by the year 2030. While 89% of the global population uses at least a basic drinking water service (round trip to collect water from an improved source takes 30min or less), only 71% of the global population uses a source that meets the Sustainable Development Goal (SDG) criteria for safely managed (accessible on premises, water available when needed, free from fecal and priority chemical contamination) ("Progress on Drinking Water, Sanitation, and Hygiene: 2017 Update and SDG Baselines," 2017). In many places, universal access to safe water is out of reach due to the high cost and lack of available financing to create and support necessary water treatment and distribution infrastructure. In some settings that have centralized treatment, leaking pipes, low water pressure, and intermittent supply contribute to recontamination during distribution (Elala, Labhasetwar, Tyrrel, & Supply, 2011; Kumpel, Nelson, & technology, 2014). Intermittent supply has been associated with increased diarrhea (Cifuentes, Suárez, Solano, & Santos, 2002; Mourad, 2004) and typhoid fever (Ercumen et al., 2015). Piped and other improved sources do not always deliver water free from contamination (Heitzinger et al., 2015; Kumpel et al., 2014; Shaheed et al., 2014); an estimated 1.4 billion people use contaminated water from improved sources ("Progress on Drinking Water, Sanitation, and Hygiene: 2017 Update and SDG Baselines," 2017). Safe and affordable drinking water for all by 2030 requires we invest in adequate infrastructure, provide sanitation facilities, and encourage hygiene (*Progress on Household Drinking water, sanitation and Hygiene*, 2021). The treatment of drinking water often involves the use of various chemicals to mitigate bacterial contamination. Commonly employed substances include free chlorine, iodine, chloramines, and ozone. While these agents are effective in disinfection, they are not without drawbacks. A significant concern is their tendency to react with natural organic matter or other substances present in water, leading to the formation of disinfection byproducts (DBPs). Some DBPs have been identified or are suspected to be carcinogenic, posing an increased risk of cancer to humans (Tessema, Gonfa, & Mekuria, 2024). This research work is aimed to design, construct, and evaluate the performance of a domestic activated sand purification device for removal of biological contaminants from polluted water suitable for rural and urban informal settlements.

2 Materials and Methods

2.1 Materials and Chemicals

The activated carbon was sourced from Panthera activated Carbon™, Silver activated sand sourced from Nikken corporation (Japan), with commercial name as Clinca205 and the zeolite was sourced from Rift African gems Kenya.

2.1.1 Leaching Test of Silver in Activated sand

A leaching test will be performed on the sample of activated sand according to the Notification No. 45(2000), "Test for materials of mechanical equipment and materials" on the basis of Ministerial ordinance No 15(2000) Japan, "Technical standards for water Utilities".

Method

Extraction procedure

The sample will be washed with flowing tap water for 1 hour, rinsed with pure water three times and then washed with a leachate (pH 7.0 ± 0.1 , hardness 45 ± 5 mg/L, alkalinity 35 ± 5 mg/L, residual chlorine 1.0 ± 0.2 mg/L) three times. Then the sample was immersed in the leachate and allowed to stand for 24 hours at 23°C. The obtained solution was used as the test water.

In addition, the leachate alone (without sample) was prepared in the same manner as the test water and used as the method blank.

The immersion rate was set at 50g of the sample per 1L of the leachate and no conditioning was performed.

2.1.2 Fourier Transform Infrared (FTIR)

The functional groups present in the different filter media was determined using a Jasco FT/IR-6600 type A

equipped with a standard light source and a triglycine sulphate (TGS) detector. The spectrum was obtained at a resolution of 4 cm^{-1} and scans ranging from a wavelength of 400 cm^{-1} to 4000 cm^{-1} .

2.1.3 X-ray Fluorescence (XRF)

The elemental composition of the filter media was determined using a Bruker CTX CounterTop XRF which has can analyze up to 48 elements per calibration, with a wide elemental range, from Mg to U.

2.1.4 Particle size analysis.

Preparation of media.

The filter media is first washed in clean water thoroughly then oven dried at 110°C for 8 hours

Particle size analysis and grading was done as per Standard Test Method for Sieve Analysis of Fine and Coarse Aggregates, ASTM C-136-06 (ASTM, 2005), where a sample of dry aggregate of known mass is separated through a series of sieves of progressively smaller openings for determination of particle size distribution.

Procedure.

1. The sample was weighed to the nearest 0.1 g by total weight of sample. This weight was used to check for any loss of material after the sample had been graded. Suitable sieve sizes were selected in accordance with the specifications.
2. The sieves were nested in order of decreasing size from top to bottom and agitation and shaking of the sample until all the media had settled in different sieve meshes was done.



FIGURE 2.1 NESTED SIEVES

3. After the material had been sieved, each tray was removed, weighed each size, and recorded each weight to the nearest 0.1 g. Care was taken to remove any aggregate trapped within the sieve openings by gently working from either or both sides with a trowel or piece of flat metal until the aggregate was freed.
4. Plot the particle distribution curve and Calculate the Uniformity Coefficient

The effective size of a given sample is the particle size (in millimeters) where 10% of the particles in that sample (by weight) are smaller, while 90% are larger. Usually this is denoted as the D10.

The size distribution is represented by the Uniformity Coefficient, which determines how well graded the sample is. This is done by taking the D60 and dividing by the D10. For slow sand filtration, some degree of uniformity is desirable in order to ensure that the pore sizes between the grains are reasonably regular and that there is sufficient porosity (Huisman & Wood, 1974).

2.2 Sample Collection and Transport

Sample collection was done according to WHO guideline procedures in order to avoid contamination and to ensure accurate results.

2.2.1 Sterilization of sample bottles

Plastic bottles of at least 200ml capacity with plastic screw caps were cleaned thoroughly, and then rinsed with distilled water and sterilized by autoclaving at 121°C for 15 minutes. Other materials used in bacteriological analysis such as dilution bottles, small cylinders, beakers, tubes, buffer solutions and pipettes were also sterilized. Water was sampled from the rivers.

2.2.2 Sampling procedures

Water samples for bacteriological analysis were collected in sterile bottles which were kept unopened until the

time of filling. The cork was removed and bottle held by the other hand around the base of the bottle. The researcher ensured that bottle was not rinsed with sample during collection and that the bottle was not completely filled to allow for shaking prior to analysis. Surface waters such as rivers were sampled away from the banks as much as possible.

2.2.3 Sampling location

Two sampling points were selected in reference to the objective of the research to provide a point of use device for rural and urban informal settlements.

The sampling points are:

1. Kesses river as shown in Fig 2.2, is a representative of a rural settlement.
2. Sosiani River as shown in Fig 2.3, represents the urban settlements.



FIGURE 2.2 KESSES RIVER SITE COORDINATES AND SAMPLING POINTS



FIGURE 2.3 SOSIANI RIVER SAMPLING SITE COORDINATES

2.3 Design of the Activated-sand based filtration unit.

The figure 2.4 shows the basic design of the POU prototype developed, whereas figure 2.5 shows the cartridges configurations used in the study.

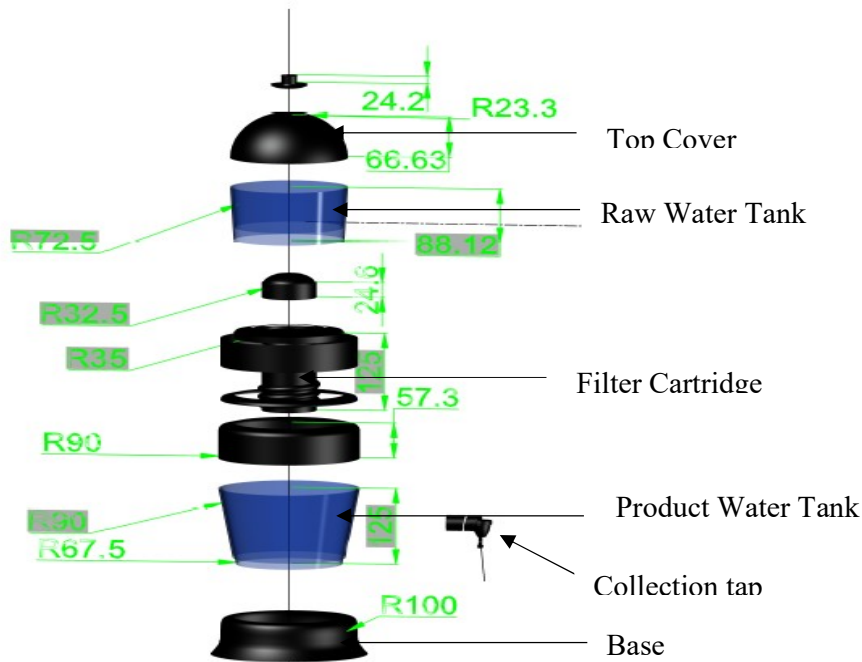


FIGURE 2.4 BASIC DESIGN OF POU WATER TREATMENT PROTOTYPE



FIGURE 2.5 CONSTRUCTED FILTER CARTRIDGE CONFIGURATIONS

Design and Construction of prototype.

Total Bed Height = 120cm

Total bed Width = 80 cm

Volume of the container

$$V = \pi r^2 h = 0.5585 \text{ cm}^3$$

Flow rate measured as 29.07 cm³/sec

$$\text{Empty bed contact time (EBCT)} = \frac{\text{Volume of media}}{\text{Flow rate}} = \frac{0.5585}{29.07} = 3.2 \text{ minutes}$$

Design of fixed bed adsorption column - Cartridge 1

The cartridge was packed with filter media as below:

Activated carbon Layer 1

Activated carbon – 97.6g
Bed height – 0.4m
Diameter – 0.77m
Adsorbent particle radius 0.92mm
Density – 290g/l

Pebbles Layer 2

Zeolite pebbles – 76.3g
Bed height – 0.2m
Diameter of the bed – 0.77m

Activated Sand Layer 3

Coarse activated sand(1180microns) – 168g
Bed height – 0.2m
Diameter of the bed – 0.77m
Density – 2.51g/cm³

Pebbles Layer 4

Zeolite pebbles – 72.7g
Bed height – 0.2m
Diameter of the bed – 0.77m

Activated Sand Layer 5

Fine activated sand(850microns) – 60g
Bed height – 0.2m
Diameter of the bed – 0.77m
Density – 2.51g/cm³

Design of fixed bed adsorption column - Cartridge 2

The cartridge was packed with filter media as below:

Activated carbon Layer 1

Activated carbon – 97.6g
Bed height – 0.4m
Diameter – 0.77m
Adsorbent particle radius 0.92mm
Density – 290g/l

Pebbles Layer 2

Zeolite pebbles – 76.3g
Bed height – 0.2m
Diameter of the bed – 0.77m

Activated Sand Layer 3

Mineral sand(1180microns) – 150g
Bed height – 0.2m
Diameter of the bed – 0.77m
Density – 2.51g/cm³

Pebbles Layer 4

Zeolite pebbles – 72.7g
Bed height – 0.2m
Diameter of the bed – 0.77m

Activated Sand Layer 5

Fine activated sand(850microns) – 60g
Bed height – 0.2m
Diameter of the bed – 0.77m
Density – 2.51g/cm³

Design of fixed bed adsorption column - Cartridge 3,4,5 (Control)

The cartridge was packed with filter media as below:

Activated carbon Layer 1

Coarse Activated carbon(>1000microns) – 97.6g
Bed height – 0.4m
Diameter – 0.77m
Adsorbent particle radius 0.92mm
Density – 290g/l
Pebbles Layer 2
Zeolite pebbles – 76.3g
Bed height – 0.2m
Diameter of the bed – 0.77m
Fine Activated Carbon Layer 3
Fine activated Carbon(<1000microns) – 40g
Bed height – 0.2m
Diameter of the bed – 0.77m
Pebbles Layer 4
Zeolite pebbles – 72.7g
Bed height – 0.2m
Diameter of the bed – 0.77m
Mineral Sand Layer 5
Mineral sand – 65g
Bed height – 0.2m
Diameter of the bed – 0.77m
Density – 2.51g/cm ³

3 Results and Discussion

3.1 XRF Analysis

The results obtained from XRF analysis of the filter materials are shown in Figure 3.1. Table 3.1 reveals that all the filter materials, contain Silica (SiO₂), Alumina (Al₂O₃), Ferric Oxide (Fe₂O₃), Calcium Oxide, Phosphorus pentoxide(P₂O₅), Chloride, Potassium Oxide and other oxides. These results compare to those of (Adekunle, Familusi, Badejo, Adeosun, & Arogundade, 2020) and (Wu, Cao, Tong, Finkelstein, & Hoek)

Activated sand and River sand show presence of MgO, which has remarkable adsorption capacity. Their unique structural properties and large surface area enable exceptional pollutant removal, including heavy metals, organic compounds, and dyes, from wastewater(Perera et al., 2024). Additionally, synthesis and functionalization techniques show promise in enhancing adsorption performance and selectivity, offering tailored solutions to specific treatment challenges. Tailoring the surface chemistry and morphology of MgO nanoparticles allows for improved pollutant removal efficiency and paves the way for tailored solutions to specific wastewater treatment challenges (Perera et al., 2024)

The presence of Silver in activated sand at 0.01%, is to act as a bactericidal to disinfect contaminated water. Bhardwaj et al. (2017) reported that the efficacy of microbial deactivation increased with the increasing concentration of silver impregnation. (Bhardwaj et al., 2018) found that the size of silver NPs is dependent on microbial killing, the highest efficiency of E. coli bacteria MIC 25 mg/L and MBC 30 mg/L have been reported in comparison to the MIC 35 mg/L and MBC 40 ppb with around 3 nm and 7 nm size of spherical shaped silver NPs, respectively.

The results also show presence of copper in all the media ranging from 0.003 to 0.066%; Copper nanoparticles have been confirmed as capable of rendering high antibacterial efficacy and hence has a great potential in the use for water disinfection(Karikalan, 2018)

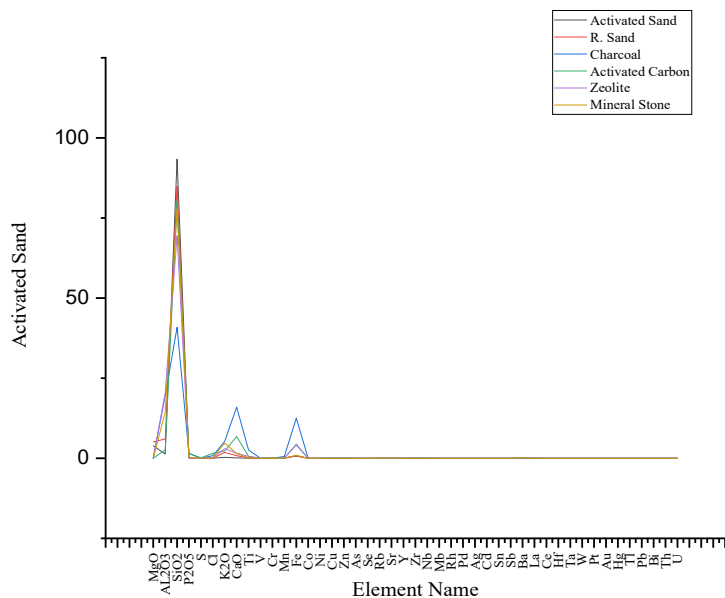


FIGURE 3.ERROR! NO TEXT OF SPECIFIED STYLE IN DOCUMENT.:1 XRF ANALYSIS OF SELECTED FILTER MEDIA

TABLE 3.1 XRF ANALYSIS OF THE FILTER MEDIA

Element Name	Activated Sand	R. Sand	Charcoal	Activated Carbon	Zeolite	Mineral Stone
MgO	3.884	5.106	-	-	-	-
AL2O3	1.353	6.038	19.569	2.622	20.468	14.388
SiO2	93.317	84.899	40.857	80.277	69.482	77.667
P2O5	0.105	0.162	1.584	1.389	-	0.179
S	0.017	-	0.041	0.11	-	-
Cl	0.055	0.055	0.819	1.51	0.111	0.123
K2O	0.295	1.839	5.258	2.234	2.997	4.75
CaO	0.124	0.812	15.959	6.791	1.591	1.448
Ti	0.026	0.097	2.603	0.598	0.613	0.158
Cr	0.057	0.018	-	0.146	0.011	0.018
Mn	0.076	0.017	0.555	0.091	0.028	0.026
Fe	0.66	0.797	12.526	4.148	4.403	0.926
Ni	-	-	-	-	0.007	-
Cu	0.005	0.004	0.012	0.066	0.009	0.003
Zn	0.002	-	0.036	-	0.007	0.002
As	-	-	0.001	-	0.001	-
Rb	0.002	0.003	0.01	-	0.018	0.022
Sr	0.002	0.039	0.045	0.017	0.008	0.061
Y	-	0.002	0.01	-	0.007	0.002
Zr	0.001	0.014	0.079	-	0.042	0.018

3.2 FTIR analysis

3.2.1 Activated Charcoal

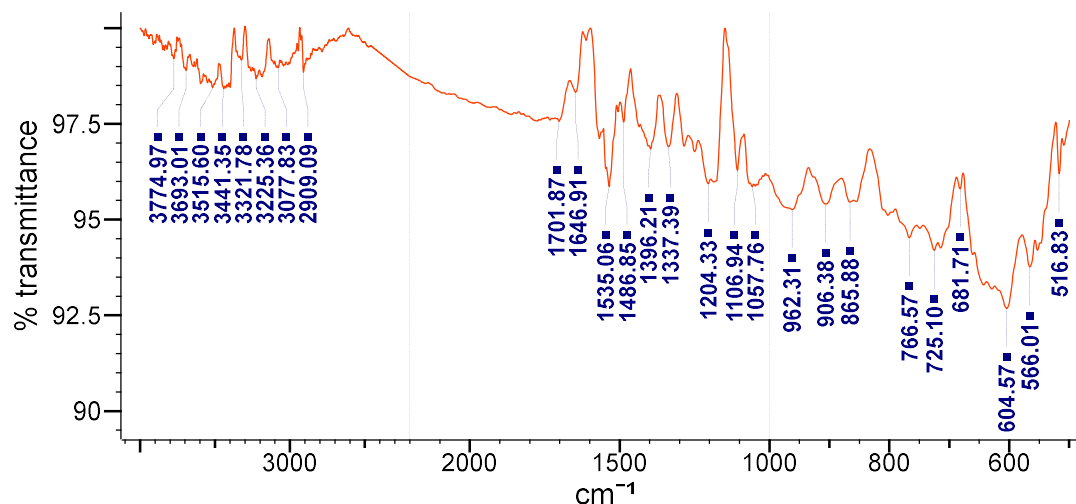


FIGURE 3.2 FTIR SPECTRA OF ACTIVATED CHARCOAL

The infrared transmission peaks recorded at a wavelength 3774.97 cm^{-1} and 3693.01 cm^{-1} exhibited a wide and broad transmission band. Here, the presence of a broad transmission band was attributed to the O-H stretching mode of non-bonded hydrogen hydroxy groups attached to the structure or surface-adsorbed moisture, this is characteristic of phenols(Nandiyanto, Oktiani, & Ragadhita, 2019). The absorption peaks at 3515.60 cm^{-1} is characteristic of Dimeric OH stretch, whereas 3441.35 cm^{-1} allude to a non polymeric OH stretch. The bands at 1057.76 cm^{-1} and 1106.94 cm^{-1} be assigned to phosphate ions(Afarinandeh, Ahmadpari, & Jahanpour, 2020); which aid in precipitate formation(Nunes, Costa, & Ortiz, 2017), whereas the peaks at 725.10 cm^{-1} , 766.57 cm^{-1} and 865.88 cm^{-1} can be assigned to the Aryl group.(Nandiyanto et al., 2019). There is also the presence of amino and organo-halogen groups.

With the major bonds being carbon or oxygen based, we can confirm that carbon and oxygen are the main elements in Activated charcoal as attributed to in the elemental analysis in Table 3.1, thus confirming its organic nature.

3.2.2 Activated Sand

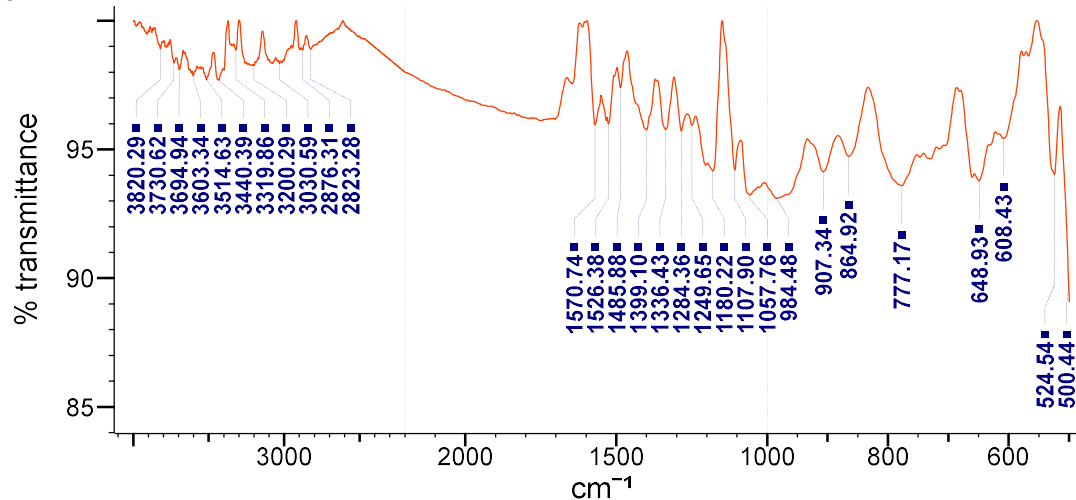


FIGURE 3.3 FTIR SPECTRA OF ACTIVATED SAND

The infrared transmission peaks recorded at the wavelengths 3603.34 cm^{-1} , 3694.94 cm^{-1} , 3730.62 cm^{-1} and 3820.29 cm^{-1} exhibited strong narrow transmission bands. Here, the presence of a narrow transmission band was attributed to the O-H stretching mode of non-bonded hydrogen hydroxy groups, this is characteristic of

phenols(Nandiyanto et al., 2019). The absorption peaks at 3514.63 cm^{-1} , 3440.39 cm^{-1} , 3319.86 cm^{-1} and 3200.29 cm^{-1} , are attributed to H-bonded with an OH stretch hydroxy group. The strong peaks at 2876.31 cm^{-1} and 2823.28 cm^{-1} are characteristic of Carboxylic acid (Rivera-Sánchez et al.) groups. The peaks at 1526.36 cm^{-1} and 1570.74 cm^{-1} are indicated for aromatic ring stretch of C=C-C bond typical of methylene. The band peaks of 1107.90 and 1180.22 are assigned to phosphate ions(Afarinandeh et al., 2020); which aid in precipitate formation(Nunes et al., 2017), whereas the peaks at 984.48 cm^{-1} and 1057.76 cm^{-1} is indicative of silicate ions(Xu, Wang, & Wu, 2024). Transmission at 1249.65 cm^{-1} is indicative of aromatic phosphates group. There is also the presence of alkenes, amino, aryl and organo-halogen groups.

The existence of phosphate and silicate ions in the activated sand, we can confirm that silica, Aluminum oxide, magnesium oxide and Potassium dioxide are the main elements in activated sand as attributed to in the elemental analysis in Table 3.1 **Error! Reference source not found.**, thus confirming its inorganic nature.

3.2.3 FTIR of Zeolite

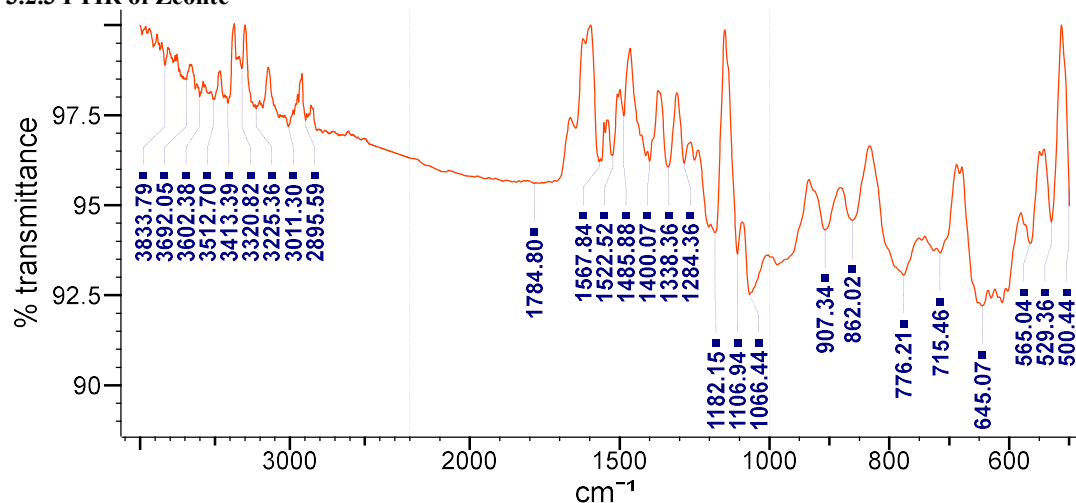


FIGURE 3.4 FTIR SPECTRA OF ZEOLITE

The infrared transmission peaks recorded at the wavelengths 3692.05 cm^{-1} and 3833.79 cm^{-1} , 3730.62 cm^{-1} and 3820.29 cm^{-1} exhibited strong narrow transmission bands. Here, the presence of a narrow transmission band was attributed to the O-H stretching mode of non-bonded hydrogen hydroxy groups, this is characteristic of phenols(Nandiyanto et al., 2019). The absorption peaks at 3602.38 cm^{-1} , 3512.70 cm^{-1} , 3413.39 cm^{-1} , 3320.82 cm^{-1} and 3225.36 cm^{-1} , are attributed to H-bonded with an OH stretch hydroxy group. The strong peaks at 2895.59 cm^{-1} and 3011.30 cm^{-1} are characteristic of Carboxylic acid (Rivera-Sánchez et al.) groups. The peaks at 1522.52 cm^{-1} and 1567.84 cm^{-1} are indicated for aromatic ring stretch of C=C-C bond typical of methylene. The weak transmission peak of 1784.80 is indicative of a simple carbonyl group e.g. Ketones, aldehydes, ester or carbonyl. The strong broad peaks exhibited at 1522.52 cm^{-1} , 1567.84 cm^{-1} and 1485.88 cm^{-1} are associated with aromatic ring stretch C=C-C bond typical of methylene. There also significant peaks at 1066.44 cm^{-1} , 1106.94 cm^{-1} and 1182.15 cm^{-1} , which are indicative of silicate ions(Xu et al., 2024). Additionally, there is the presence of alkenes, aryl and organo-halogen groups.

From the existence of silicate ions in the zeolite, we can confirm that silica and Aluminum oxide are the main elements in zeolite, as attributed to in the elemental analysis in Table 3.1 XRF analysis of the filter media **Error! Reference source not found.**, thus confirming its inorganic nature.

3.3 Bacteriological removal

3.3.1 Removal of Total Coliforms in the cartridge filter.

The cartridge filter is highly efficient in removal of total coliform from contaminated water. The average performance of filter cartridge 1 was 100% whereas that of filter 2 was 99%, for water samples obtained from Kesses river. The average removal efficiency was 100% on filter 1 and 99.6% for water samples obtained from Sosiani river. Potable water shall be free of any total coliform bacteria (WHO., Organization, & Staff, 2004) (Standards, 2015). The Total Coliform in drinking water range from 1 to 10 (CFU/100 ml) is called “a reasonable quality”, 11 to 100 FC (CFU/100 ml) is in “polluted” range, 101 to 1000 FC (CFU/100 ml) is “dangerous” range, while over 1000 FC (CFU/100 ml) is called “a very dangerous” range (WHO. et al., 2004). The average Total

Coliform removal performance of sand based filter cartridges ranges from 33.7% to 96.1%(Nassar & Hajjaj, 2013; Tiwari, Schmidt, Darby, Kariuki, & Jenkins, 2009). The results obtained from this study agree with those of Das T.K, et al who reported total coliform reduction of 91.52%(Das, Shaibur, Shalihin, & Mamun) and (Ndebele, 2020), reported 100% removal.

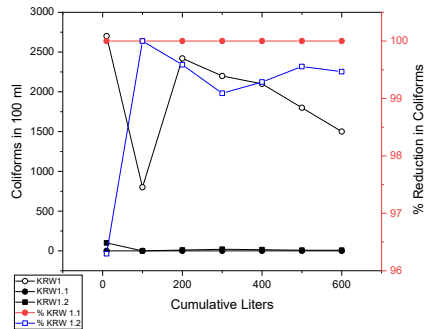


FIGURE 3.5 REDUCTION IN TOTAL COLIFORMS IN KESSES RIVER WATER

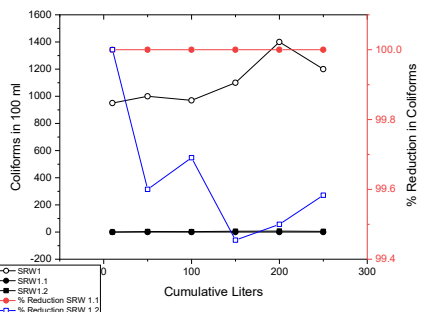


FIGURE 3.6 REDUCTION IN TOTAL COLIFORMS IN SOSIANI RIVER WATER

3.3.2 Removal of *Streptococcus faecalis* in the cartridge filter.

The removal efficiency of *S. faecalis* from the two water sources by the filter cartridge configuration 1 and 2 are as shown in figure 3.7 and 3.8. The removal efficiency was however higher in filter cartridge 1 averaging 100% whereas that of cartridge 2 averaged 99.9%, on Kesses river water which had a higher loading rate of *S. faecalis* pathogens as compared to sosiani river water. The silver concentration is attributed to the inhibition of the highly resistant viral indicators (bacteriophages), and explains the disparity in removal efficiency between cartridge 1 and 2, with cartridge 1 having a higher concentration of silver. The results of this study agree with those of (Adler, 2014) who achieved total elimination of *S. faecalis* in his model in one minute. Similar studies have shown 94.7% reduction (Ndebele, 2020), whereas Meierhofer, et al while assessing the effect of activated silver on water quality reported total inactivation of *S. faecalis*(Meierhofer, Rubli, Oremo, & Odhiambo, 2019).

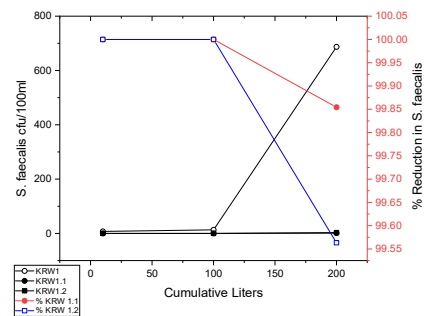


FIGURE 3.7 REMOVAL EFFICIENCY OF S. FAECALIS ON KESSES RIVER WATER

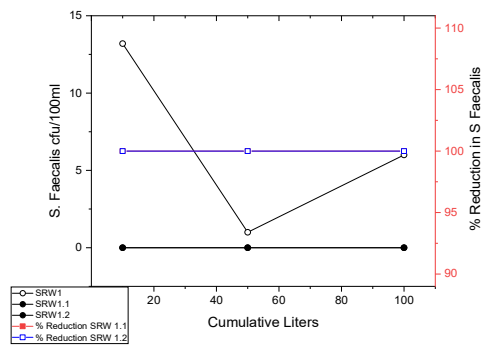


FIGURE 3.8 REMOVAL EFFICIENCY OF S. FAECALIS ON SOSIANI RIVER WATER

Factor Coding: Actual

S. FAECALIS
 (adjusted for curvature)

Design Points
 0 100

X1 = D
 X2 = A

Actual Factors
 B = 43.75
 C = 210
 E = 1210

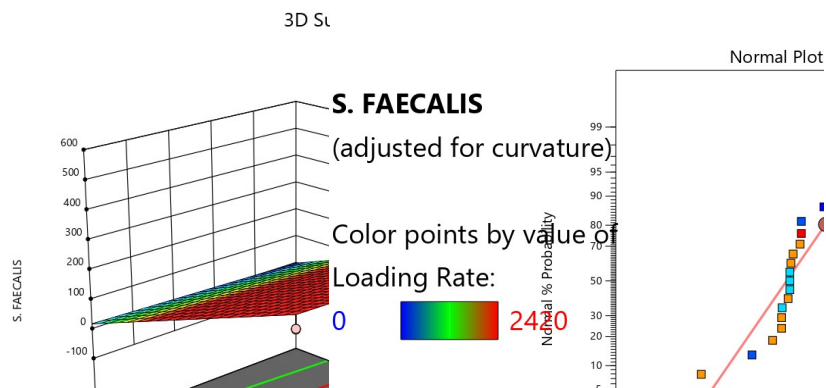


FIGURE 3.10 NORMAL S.FAECALIS PROBABILITY

FIGURE 3.9 3D GRAPH SURFACE OF FAECALIS

On analysis of *S.faecalis* variable on Design Expert 13, the optimized solution was of sand concentration of 25g/l and grain size of 1015 microns as shown in Figure 3.9 3d graph surface of faecalis. The removal efficiency *s.faecalis* is expressed as the actual response value. The number of actual response value data obtained is 20 data and is completed in

Table 3.3 anova model on s.FAECALIS on Design Expert 13 software for statistical analysis. Statistical analysis was carried out using the Analysis of Variance (ANOVA) to determine whether there was an effect of the variables used the filter cartridge.

TABLE 3.2 FIT STATISTICS S. FAECALIS

Std. Dev.	16.17	R²	0.6903
Mean	14.75	Adjusted R²	0.4933
C.V. %	109.63	Predicted R²	0.4877
		Adeq Precision	6.6276

The ANOVA of S. Faecalis Table 3.2 Fit statistics s. faecalis, shows that the correlation coefficient (R^2) is 0.69. These results indicate that the relationship between variables and data is strong (Fitriani, Wahyudianto, Salsabila, Mohamed, & Kurniawan, 2023), because R^2 value is close to one. This is reinforced by the results of Adeq precision of 6.63, is higher than 4 (Oyekanmi et al., 2019), which are the desired model results.

TABLE 3.3 ANOVA MODEL ON S.FAECALIS

Source	Sum of Squares	df	Mean Square	F-value	p-value	
Model	6411.77	7	915.97	3.50	0.0314	significant
A-Grain Size	2639.88	1	2639.88	10.10	0.0088	
B-Flow Rate	626.48	1	626.48	2.40	0.1499	
D-Sand Concentration	384.01	1	384.01	1.47	0.2509	
E-Loading Rate	2205.44	1	2205.44	8.44	0.0143	
AE	2659.43	1	2659.43	10.17	0.0086	
BD	958.73	1	958.73	3.67	0.0819	
DE	703.89	1	703.89	2.69	0.1291	
Curvature	2813.89	1	2813.89	10.76	0.0073	
Residual	2876.08	11	261.46			
Lack of Fit	2869.33	8	358.67	159.41	0.0007	significant
Pure Error	6.75	3	2.25			
Cor Total	12101.75	19				

Factor coding is **Coded**.

Sum of squares is **Type III - Partial**

The **Model F-value** of 3.50 implies the model is significant. There is only a 3.14% chance that an F-value this large could occur due to noise.

P-values less than 0.0500 indicate model terms are significant. In this case A, E, AE are significant model terms. Values greater than 0.1000 indicate the model terms are not significant.

4.3.3 Removal of Shigella in the cartridge filter.

The sample water collected from the Kesses and Sosiani river showed zero levels of Shigella, however those obtained from Boundary River water detected Shigella whose data is now reported on Figure 3.11 removal efficiency of Shigella. The method of analysis of Shigella was be detection and not enumeration (Coded 1 – Detected(D) and 2- Not detected (ND)).

The removal efficiency in both cartridge filters was 100%, this results are similar to the study by Rashid et al who managed Shigella removal rates of 85% (Rashid, Salman, & Mohammed, 2021).

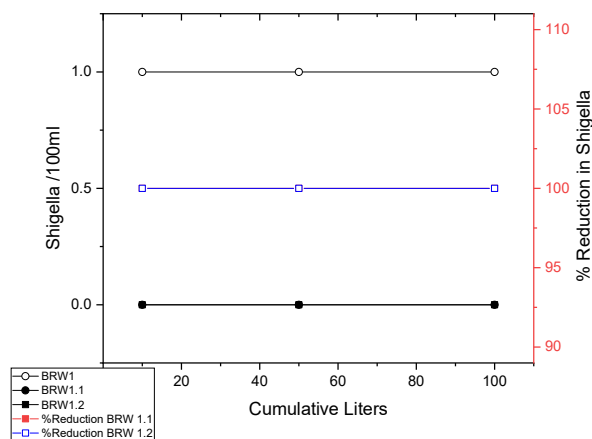


FIGURE 3.11 REMOVAL EFFICIENCY OF SHIGELLA

3.3.4 Reduction of Salmonella in the cartridge filter.

The removal efficiency of salmonella from Sample water from Kesses and Sosiani rivers by cartridge 1 and 2

showed salmonella reduction of 100% figure 3.12, this compares with a previous study Rivera-Sanchez et al who reported removal efficiency of 99.98% (Rivera-Sánchez et al., 2020) and Perez-Vidal, et al reported reduction of 1 LRV in salmonella spp. (Pérez-Vidal et al., 2019).

The basis of measurement of Salmonella was by detection (1- Detected and 2- Not Detected)

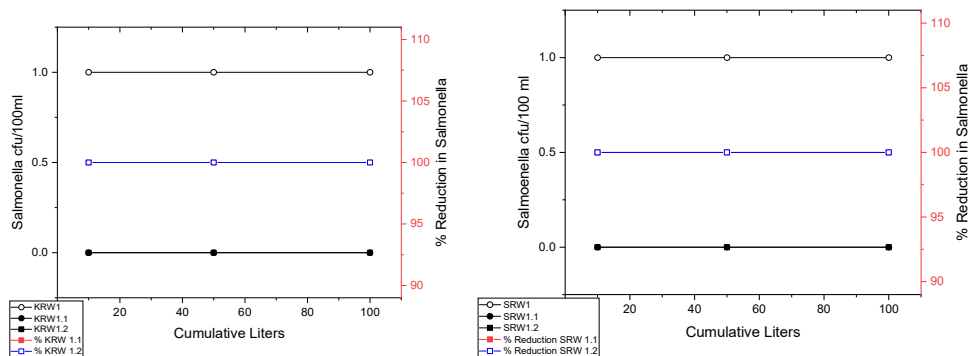


FIGURE 3.12 REMOVAL EFFICIENCY OF SALMONELLA

Mechanism of silver particles on pathogenic Contaminants.

Silver particles have various antibacterial effects, but their exact mechanisms of action are unknown. They release silver ions that can stop bacteria from growing by binding to sulphur containing proteins and amino acids in bacterial cell membranes leads to inactivation of the bacteria on their membranes and walls. Additionally, the release of silver ions from Silver particles can inhibit enzyme activities by interacting with phosphorus in DNA and sulphur in proteins Silver particles are also indeed known for attributed to their ability to interact with negatively charged biomolecules. When silver particles come into contact with bacterial cells, they can attach to the cell membrane due to electrostatic attraction, as the cell membrane often carries a negative charge. This interaction can lead to the disruption of the cell membrane's integrity, causing structural changes that can ultimately result in cell death. Additionally, Silver particles can penetrate inside the bacteria, where they may interact with sulfur-containing proteins and phosphorus-containing elements like DNA, leading to further damage. These interactions can inhibit cell replication and lead to the generation of reactive oxygen species, which can also contribute to the bactericidal effect of silver particles (Mukundan, Mohankumar, & Vasanthakumari, 2017; Tessema et al., 2024).

The precise mechanisms of action are complex and still under investigation, but the ability of silver particles to induce multiple types of damage to bacterial cells is a key factor in their antimicrobial efficacy

4. Conclusion

Through FTIR and XRF analysis the filter media was confirmed to contain Silver, MgO, SiO₂, Al₂O₃ and Copper. The Silver particles release silver ions that can stop bacteria from growing by binding to sulphur containing proteins and amino acids in bacterial cell membranes leads to inactivation of the bacteria on their membranes and walls, whereas MgO, which has remarkable adsorption capacity and unique structural properties with large surface area enable exceptional pollutant removal, including heavy metals and organic compounds. Silicon dioxide SiO₂, is known for antibacterial effect against E.coli and is used for reusable antibacterial inactivation, Aluminium Silicate (Al₂O₃), is a good coagulant, whereas copper has greater virus removal efficacy at reduced cost, making it viable for water filter development.

The baseline water quality experiments showed variation of water quality parameters with the amount of precipitation received, this were attributed to surface runoff from the agricultural farms around increasing the chemical and biological concentrations of contaminants.

The prototype design iterations came up with a multi-layer bed consisting of five layers of filter media packed to facilitate contaminant removal at each layer, at a designed flow rate, residence time and concentration. It is so designed that at the bottom of the bed is silver-activated sand, that is continually in contact with product water to ensure for residual disinfection.

The biological removal efficiencies observed were Salmonella 100%, Shigella 100%, *S. faecalis* 100%, 99.9%, Total Coliforms 100%, 99% for filter cartridge 1 and 2 respectively.

The silver-activated water purification system offers an effective and sustainable solution for improving household water quality. By leveraging the antimicrobial properties of silver, this system addresses critical public health concerns related to waterborne diseases.

The long-term impact of silver on health and the environment is still a subject of ongoing research, while silver has proven antibacterial properties, excessive accumulation and consumption could pose risks. Hence, monitoring and managing silver release from filters is essential to mitigate any potential adverse effects. The silver release to the effluent was monitored and the average result was 0.02mg/l, which is lower than the recommended 0.1mg/l by the World health organization.

In Conclusion the silver-activated water purification system offers an effective and sustainable solution for improving household water quality. As communities continue to face challenges related to water scarcity and quality, such innovative solutions hold promise for enhancing access to safe drinking water globally.

This system addresses significant public health problems associated with waterborne diseases, using zero energy making it affordable, sustainable and attractive to both the urban and rural settlement usage. It is therefore recommended for commercialization in order to benefit the wider community.

Acknowledgements

The authors acknowledge the African Centre of Excellence in Phytochemicals, Textiles and Renewable Energy (ACEII-PTRE) for funding this research, Nikken Corporation Japan for the supply of activated sand, Panthera Carbon™, Rift African gems, the department of civil engineering for providing a working space, The Kenya bureau of standards(KEBS), Eldoret water and sanitation company(ELDOWAS) and the Ministry of mining, Kenya.

References

- Adekunle, A. A., Familusi, A. O., Badejo, A. A., Adeosun, O. J., & Arogundade, S. A. (2020). Characterisation of activated charcoal, sawdust charcoal and rice husk charcoal as adsorbents in water treatment. *Analecta Technica Szegedinensia*, 14(2), 19-25.
- Adler, I. (2014). *Application of filtration and silver-ion based disinfection to purify rainwater for potable uses in rural communities of Mexico*. UCL (University College London),
- Afarinandeh, A., Ahmadpari, H., & Jahanpour, A. (2020). Investigation of Chemical Coagulation and Flocculation Efficiency of Different Coagulants in Phosphorus pentoxide and Fluoride Removal from Kimia Daran Kavir Factory Wastewater. *Journal of Biochemical Technology*, 11(1-2020), 30-40.
- ASTM. (2005). Standard Test Method for Sieve Analysis of Fine and Coarse Aggregates. In.
- Bhardwaj, A. K., Shukla, A., Maurya, S., Singh, S. C., Uttam, K. N., Sundaram, S., . . . Gopal, R. (2018). Direct sunlight enabled photo-biochemical synthesis of silver nanoparticles and their Bactericidal Efficacy: Photon energy as key for size and distribution control. *Journal of Photochemistry and Photobiology B: Biology*, 188, 42-49.
- Cifuentes, E., Suárez, L., Solano, M., & Santos, R. J. E. H. P. (2002). Diarrheal diseases in children from a water reclamation site in Mexico city. *110(10)*, A619-A624.
- Das, T., Shaibur, M., Shalihin, R., & Mamun, A. PERFORMANCE EVALUATION OF BIO-SAND FILTER IN REMOVING CONTAMINATS FROM SURFACE WATER. *Journal of Jessore University of Science and Technology ISSN*, 2521, 5493.
- Drinking Water FactSheet*. (2019). Retrieved from
- Elala, D., Labhasetwar, P., Tyrrel, S. F. J. W. S., & Supply, T. W. (2011). Deterioration in water quality from supply chain to household and appropriate storage in the context of intermittent water supplies. *11(4)*, 400-408.
- Ercumen, A., Arnold, B. F., Kumpel, E., Burt, Z., Ray, I., Nelson, K., & Colford Jr, J. M. J. P. m. (2015). Upgrading a piped water supply from intermittent to continuous delivery and association with waterborne illness: a matched cohort study in urban India. *12(10)*, e1001892.
- Fitriani, N., Wahyudianto, F. E., Salsabila, N. F., Mohamed, R. M. S. R., & Kurniawan, S. B. (2023).

- Performance of modified slow sand filter to reduce turbidity, total suspended solids, and iron in river water as water treatment in disaster areas. *Journal of Ecological Engineering*, 24(1).
- Heitzinger, K., Rocha, C. A., Quick, R. E., Montano, S. M., Tilley Jr, D. H., Mock, C. N., . . . hygiene. (2015). "Improved" but not necessarily safe: an assessment of fecal contamination of household drinking water in rural Peru. 93(3), 501.
- Huisman, L., & Wood, W. E. (1974). *Slow sand filtration*: World Health Organization.
- Karikalan, N. (2018). Synthesis and characterization of copper nanoparticles and evaluation of antibacterial activity. *Rasayan J Chem*, 11(4), 1451-1457.
- Kumpel, E., Nelson, K. L. J. E. s., & technology. (2014). Mechanisms affecting water quality in an intermittent piped water supply. 48(5), 2766-2775.
- Meierhofer, R., Rubli, P., Oremo, J., & Odhiambo, A. (2019). Does activated silver reduce recontamination risks in the reservoirs of ceramic water filters? *Water*, 11(5), 1108.
- Mourad, T. A. J. P. h. (2004). Palestinian refugee conditions associated with intestinal parasites and diarrhoea: Nuseirat refugee camp as a case study. 118(2), 131-142.
- Mukundan, D., Mohankumar, R., & Vasanthakumari, R. (2017). Comparative study of synthesized silver and gold nanoparticles using leaves extract of *Bauhinia tomentosa* Linn and their anticancer efficacy. *Bulletin of Materials Science*, 40, 335-344.
- Nandiyanto, A. B. D., Oktiani, R., & Ragadhita, R. (2019). How to read and interpret FTIR spectroscopy of organic material. *Indonesian Journal of Science and Technology*, 4(1), 97-118.
- Nassar, A. M., & Hajjaj, K. (2013). Purification of stormwater using sand filter. *Journal of Water Resource and Protection*, 5(11), 1007-1012.
- Ndebele, N. (2020). *Assessment of the use of ceramic water filters with silver nitrate as point-of-use water treatment devices in Dertig, North West Province, South Africa*.
- Nunes, R. M., Costa, D., & Ortiz, N. (2017). The use of eucalyptus activated biocarbon for water treatment-adsorption processes. *American Journal of Analytical Chemistry*, 8(8), 515-522.
- Oyekanmi, A. A., Daud, Z., Mohamed, R. M. S. R., Ab Aziz, N. A., Ismail, N., Rafatullah, M., . . . Hossain, K. (2019). Adsorption of pollutants from palm oil mill effluent using natural adsorbents: Optimization and isotherm studies. *Desalination and Water Treatment*, 169, 181-190.
- Perera, H., Gurunathanan, V., Singh, A., Mantilaka, M., Das, G., & Arya, S. (2024). Magnesium oxide (MgO) nano-adsorbents in wastewater treatment: A comprehensive review. *Journal of Magnesium and Alloys*.
- Pérez-Vidal, A., Rivera-Sánchez, S. P., Florez-Elvira, L. J., Silva-Leal, J. A., Diaz-Gomez, J., Herrera-Cuero, L. F., & Botero, L. P. L. (2019). Removal of *E. coli* and *Salmonella* in pot ceramic filters operating at different filtration rates. *Water Res*, 159, 358-364.
- Progress on Drinking Water, Sanitation, and Hygiene: 2017 Update and SDG Baselines. (2017). *World Health Organization (WHO) & United Nations Children's Fund (UNICEF)*. Retrieved from <http://www.who.int/mediacentre/news/releases/2017/launch-version-report-jmpwater->
- Progress on Household Drinking water, sanitation and Hygiene*. (2021). Retrieved from
- Rashid, I. M., Salman, S. D., & Mohammed, A. K. (2021). Removal of pathogenic bacteria from synthetic contaminated water using packed bed silver nanoparticle-coated substrates. *Energy, Ecology and Environment*, 6, 462-468.
- Rivera-Sánchez, S. P., Ocampo-Ibáñez, I. D., Silva-Leal, J. A., Flórez-Elvira, L. J., Castaño-Hincapié, A. V., Dávila-Estupiñan, A., . . . Pérez-Vidal, A. (2020). A novel filtration system based on ceramic silver-impregnated pot filter combined with adsorption processes to remove waterborne bacteria. *Scientific Reports*, 10(1), 11198.
- Shaheed, A., Orgill, J., Ratana, C., Montgomery, M. A., Jeuland, M. A., Brown, J. J. T. M., & Health, I. (2014). Water quality risks of 'improved' water sources: evidence from Cambodia. 19(2), 186-194.
- Sila, O. N. a. (2018). Physico-chemical and bacteriological quality of water sources in rural settings, a case study of Kenya, Africa. *Elsevier*, 2(e00018), 13.
- Standards, K. B. o. (2015). Potable Water - Specification. In: KEBS.
- Tessema, B., Gonfa, G., & Mekuria, S. (2024). Preparation of modified silica gel supported silver nanoparticles and its evaluation using zone of inhibition for water disinfection. *Arabian Journal of Chemistry*, 106036.
- Tiwari, S. S. K., Schmidt, W. P., Darby, J., Kariuki, Z., & Jenkins, M. W. (2009). Intermittent slow sand filtration for preventing diarrhoea among children in Kenyan households using unimproved water sources: randomized controlled trial. *Tropical Medicine & International Health*, 14(11), 1374-1382.
- water.org/. (2021). [water.org/our-impact/where-we-work/kenya/](http://www.water.org/our-impact/where-we-work/kenya/). Retrieved from www.water.org/our-impact/where-we-work/kenya/
- WHO., Organization, W. H., & Staff, W. H. O. (2004). *Guidelines for drinking-water quality* (Vol. 1): World health organization.
- Wright, J., Gundry, S. & Conroy, S. 2003. (2003). Household drinking water in developing countries: A

- systematic review of microbiological contamination between source water and point of use. *Tropical Medicine International Health*, 9, 106-117.
- Wu, J., Cao, M., Tong, D., Finkelstein, Z., & Hoek, E. M. J. n. C. W. (2021). A critical review of point-of-use drinking water treatment in the United States. *4*(1), 1-25.
- Xu, M., Wang, J., & Wu, J. (2024). Recent advances of silicate materials for wastewater treatment: a review. *Materials Research Express*.